Tsai, I.-H., Prasanna Murthy, S. N., & Steck, T. L. (1982) *J. Biol. Chem. 257*, 1438–1442.
Tudhope, G. R., & Hopkins, J. (1974) *Clin. Sci. Mol. Med. 46*, 635–645.
Walder, J. A., Walder, R. Y., & Arnone, A. (1980) *J. Mol. Biol. 141*, 195–216.
Walder, J. A., Chatterjee, R., Steck, T. L., Low, P. S., Musso, G. F., Kaiser, E. T., Rogers, P. H., & Arnone, A. (1984) *J. Biol. Chem. 259*, 10238–10246.
Waugh, S. M., & Low, P. S. (1985) *Biochemistry 24*, 34–39.
Waugh, S. M., Willardson, B. M., Kannan, R., Labotka, R. J., & Low, P. S. (1986) *J. Clin. Invest. 78*, 1155–1160.
Wiedenmann, B., & Elbaum, D. (1983) *J. Biol. Chem. 258*, 5483–5489.
Winterbourn, C. C., & Carrell, R. W. (1974) *J. Clin. Invest. 54*, 678–689.
Wyman, J. (1964) *Adv. Protein Chem. 19*, 223–286.
Zilber, I., & Shaklai, N. (1982) *Biochem. Int. 4*, 297–303.

Determination of the Depth of Bromine Atoms in Bilayers Formed from Bromolipid Probes†

T. J. McIntosh*
Anatomy Department, Duke University Medical Center, Durham, North Carolina 27710
Peter W. Holloway*
Department of Biochemistry, University of Virginia School of Medicine, Charlottesville, Virginia 22908
Received June 10, 1986; Revised Manuscript Received November 18, 1986

ABSTRACT: X-ray diffraction analysis has been performed on a series of 1-palmitoyl-2-dibromostearoylphosphatidylcholines (BRPCs) with bromine atoms at the 6,7-, the 11,12-, or the 15,16-positions on the *sn*-2 acyl chains. The diffraction patterns indicate that, when hydrated, each of these lipids forms liquid-crystalline bilayers at 20 °C. For each lipid, electron density profiles and continuous Fourier transforms were calculated by the use of swelling experiments. In the electron density profiles, high-density peaks, due to the bromine atoms, are observed. The separation between these bromine peaks in the profile decreases as the bromine atoms are moved toward the terminal methyl of the acyl chain. For the 6,7- and 11,12-bromolipids, experimental Fourier transforms can be approximated by the sum of the transform of 1-palmitoyl-2-oleoylphosphatidylcholine (POPC) and the transform of two symmetrically placed peaks of electron density (the bromines). For the case of the 15,16-bromolipids, a better fit is obtained for the transforms of a model bilayer where the thickness of the methylene chain region of the bilayer is 3 Å greater than that of POPC. Our analysis indicates the following: (1) for each of these bromolipids, the bromines are well localized in the bilayer; (2) the distance of the bromines from the head-group–hydrocarbon boundary are 3.5, 8.0, and 14 Å, for 6,7-, 11,12-, and 15,16-BRPC, respectively; (3) the bilayer thickness and perturbation to bilayer hydrocarbon chain packing caused by the bromine atoms depend on the position of the bromines on the hydrocarbon chain.

Although many important functions are associated with cell membranes, our understanding of these processes has been hampered by the lack of high-resolution techniques for determining the three-dimensional structure of membrane proteins (Eisenberg, 1984), and only recently has there been a complete X-ray crystallographic analysis of an integral membrane protein (Deisenhofer et al., 1985). Both X-ray and neutron diffraction have been applied to membrane proteins in partially ordered structures, for example, cytochrome b_5 in oriented stacks of membranes, and in these studies, the resolution is sufficient to locate the protein mass within the bilayer (Gogol & Engelman, 1984; Rzepecki et al., 1986). Low-resolution structural information on membrane proteins can also be obtained by nuclear magnetic resonance (Smith & Oldfield, 1984) and by fluorescence techniques, the latter having the advantage that fluorescence is inherently very sensitive. Three recent reports and reviews (London, 1982; Kleinfeld, 1985; Blatt & Sawyer, 1985) have described the use of fluorescence quenching or fluorescence energy transfer to determine the structure, and other properties, of membrane proteins. These techniques have been most commonly used to determine the depth of protein-bound fluorophores within the membrane bilayer.

To determine the depth of the fluorophore, a series of probes which have a quencher or energy acceptor attached to different positions of a hydrocarbon backbone is used. The spin-labeled fatty acids (London, 1982) or the anthroyloxy fatty acids (Kleinfeld, 1985; Blatt & Sawyer, 1985) are commonly used. These probes are incorporated into membranes which also contain the protein under investigation. The simple assumption is that the most efficient quenching or energy transfer will occur when the quencher or acceptor and the protein fluorophore are at the same depth in the membrane. The extrapolation of this type of observation to a prediction of the depth of the protein-bound fluorophore requires that the depth of the quencher or acceptor be precisely known. The depths, in the membrane, of the spin-labeled fatty acid quenchers and the anthroyloxy-labeled fatty acid acceptors have been determined by a variety of techniques [reviewed in London

†This work was supported by NIH Grants GM23858 (to P.W.H.) and GM27278 (to T.J.M.).

0006-2960/87/0426-1783$01.50/0

(1982) and Blatt & Sawyer (1985)]. Many of these techniques are rather indirect, have used higher probe concentrations than are usually used in fluorescence measurements, and are not very precise.

In our ongoing studies of cytochrome b_5, we have synthesized a series of brominated phosphatidylcholines (BRPC),[1] with bromine atoms at different positions on the *sn*-2 acyl chain (Markello et al., 1985; Everett et al., 1986). These lipids have been used to determine the depth, in the membrane, of the fluorescent tryptophan which resides in the membrane binding domain of the cytochrome. Other groups have also used brominated lipids as fluorescence quenchers (East & Lee, 1982; Ludi et al., 1985; Jain & Maliwal, 1985). The use of BRPCs as quenchers overcomes many of the problems associated with other quenching species. The membrane can be made completely from BRPC, and so the problems of the location of the quencher in the lateral plane of the membrane are avoided. Partitioning between aqueous and membrane compartments (Everett et al., 1986) and movement from one monolayer to the other, which is seen with anthroyloxy fatty acids (Storch & Kleinfeld, 1986), will not occur, and finally, bromine atoms would be expected to be minimally perturbant of the membrane. In support of this last assumption, it was shown that dimensions of sonicated vesicles prepared from BRPCs were similar to those prepared from 1-palmitoyl-2-oleoylphosphatidylcholine (POPC) (Markello et al., 1985). Although the precise mechanism of quenching of BRPCs is not known, they, like the spin-labeled quenchers (London, 1982), act over a very short distance, in contrast to the long-range effects of the energy-transfer quenchers. As a result, a membrane-bound fluorophore will only be quenched by lipid molecules in its immediate environment. In our previous studies with cytochrome b_5, we suggested that this property would enable the determination of the depth of tryptophans of this protein relative to the immediate lipid environment and so locate this protein relative to its "boundary lipid" (Markello et al., 1985). Finally, a major advantage of bromine as a quencher is its high electron density, which enables the position of bromine atoms in the membrane to be determined by X-ray techniques (Franks et al., 1978; Lytz et al., 1984).

This report uses X-ray techniques to determine the bilayer structure and localization of the bromine atoms for three lipids with bromines at different positions along the hydrocarbon chains. The lipids studied are 1-palmitoyl-2-dibromostearoylphosphatidylcholines (BRPCs) with the bromines located at the 6- and 7-positions (6,7-BRPC), 11- and 12-positions (11,12-BRPC), and 15- and 16-positions (15,16-BRPC). Our analysis indicates that all of these lipids form bilayers with the bromine atoms well localized in the hydrocarbon regions. The approximate distances of the pair of bromines from the bilayer centers are 11, 6.5, and 2 Å for 6,7-BRPC, 11,12-BRPC, and 15,16-BRPC, respectively. The dimensions of the bilayer also depend on the location of the bromine atoms. The bilayer widths are the same to within 1 Å for POPC, 6,7-BRPC, and 11,12-BRPC. However, the width of the 15,16-BRPC bilayer is about 3 Å wider than the POPC bilayer.

These results confirm our previous conclusions as to the location of the tryptophans of cytochrome b_5 (Markello et al., 1985; Everett et al., 1986). In addition, we suggest that these brominated lipids could be used to "calibrate" other probe molecules which could then be used as "secondary" standards in depth measurements on membrane proteins.

[1] Abbreviations: PC, phosphatidylcholine; POPC, 1-palmitoyl-2-oleoylphosphatidylcholine; BRPC, 1-palmitoyl-2-dibromostearoylphosphatidylcholine; 6,7-, 11,12-, and 15,16-BRPC, BRPC with the bromine atoms at the designated positions.

Materials and Methods

Synthesis of Brominated Lipids. The different 1-palmitoyl-2-dibromostearoylphosphatidylcholines were prepared and characterized as described previously (Markello et al., 1985). In brief, the corresponding octadecenoic acid was converted to the dibromide which was then used to reacylate 1-palmitoylglycerophosphocholine by the procedure of Boss et al. (1975). The 6- and 11-octadecenoic acids were obtained from Nu Check Prep Inc., Elysian, MN. The 15-octadecenoic acid was prepared from *cis*-11-tetradecenol (Sigma Chemical Co., St. Louis, MO) by two cycles of malonic ester synthesis. By differential scanning calorimetry, the 6,7- and 11,12-BRPCs had no phase transitions between 5 and 50 °C, whereas the 15,16-BRPC had a broad transition centered at 14 °C.

X-ray Diffraction. Specimens for X-ray diffraction analysis were made by adding measured amounts of triply distilled water, in the range of 10–40% by weight, to dry lipid in a conical glass reaction vial. These suspensions were covered with nitrogen, sealed, and allowed to equilibrate at room temperature for at least 24 h. The specimens were then sealed in a quartz glass X-ray capillary tube and mounted in a pinhole collimation X-ray camera with three or more sheets of Kodak DEF-5 X-ray film in a flat-plate film cassette. The specimen to film distance was 10 cm, and exposure times were between 5 and 15 h. All experiments were performed at ambient temperatures, 20 ± 2 °C. Films were processed by standard techniques and densitometered with a Joyce-Loebl microdensitometer, Model MK IIIC. The background curve was subtracted and integrated intensities, $I(h)$, where h is the diffraction order, were obtained as previously described (McIntosh, 1980). For these experiments with unoriented suspensions, the structure amplitude, $|F(h)|$, for each order h was set equal to $[h^2I(h)]^{1/2}$. Continuous transforms were calculated by use of the sampling theorem (Shannon, 1949; Worthington et al., 1973). For the BRPCs, the values of the structure amplitudes at the origin of reciprocal space were calculated by the formalism of King and Worthington (1971). The phase angles and value of $F(0)$ used for POPC were equivalent to those determined for egg phosphatidylcholine (Torbet & Wilkins, 1976; McIntosh & Simon, 1986), since the intensity distribution and repeat periods are very similar for these two lipids.

Results

For all lipids studied, POPC, 6,7-BRPC, 11,12-BRPC, and 15,16-BRPC, the X-ray diffraction patterns consist of 4–6 orders of a lamellar repeat period and a single broad wide-angle band centered at approximately 4.5 Å. This means that, at 20 °C, these lipids all form liquid-crystalline lipid bilayers (Tardieu et al., 1973). The repeat period and intensity distribution both depend on the type of lipid and water content. Structure factors for a series of swelling experiments for 6,7-, 11,12-, and 15,16-BRPC are shown as closed circles in Figure 1. For each lipid, there are several sets of structure factors corresponding to repeat periods obtained at different water contents. For each of these lipids, the phase angles were determined, as done previously (McIntosh et al., 1983, 1984; Blaurock & McIntosh, 1986), by calculating continuous transforms (Shannon, 1949) for each data set, for each possible phase combination, and choosing the phase combination which gave the closest agreement among the transforms. The solid lines in Figure 1 are the mean of the transforms calculated for all data sets with the correct phase combination, and the

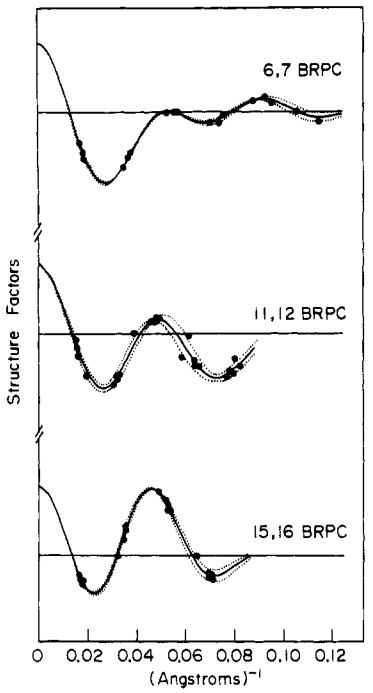

FIGURE 1: Structure factors and continuous Fourier transforms for 6,7-, 11,12-, and 15,16-BRPC. The circles represent observed structure factors for a series of swelling experiments—3, 5, and 5 data sets for 6,7-BRPC, 11,12-BRPC, and 15,16-BRPC, respectively. The solid curves are mean values of transforms for these data sets, and the dotted curves show ±1 standard deviation.

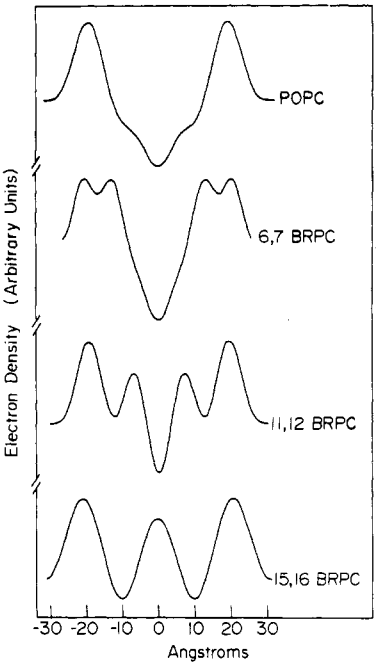

FIGURE 2: Electron density profiles for POPC, 6,7-BRPC, 11,12-BRPC, and 15,16-BRPC. The geometric center of each bilayer is at the origin (0 Å).

dotted lines represent plus and minus 1 standard deviation calculated at each point in reciprocal space. The transforms for 6,7-BRPC extend to higher values of reciprocal space than the other lipids, since more diffraction orders were recorded with this lipid. Notice that the shape of the transform varies considerably as a function of position of the bromine atoms on the hydrocarbon chains (Figure 1).

Figure 2 shows typical electron density profiles for POPC, 6,7-BRPC, 11,12-BRPC, and 15,16-BRCP. For each profile, the geometric center of the bilayer is at the origin, 0 Å, and the high-density peaks centered at about ±20 Å correspond to the lipid head groups. Electron density profiles calculated by using all of the data sets presented in Figure 1 give the following values for the distance (mean ± standard deviation) between head-group peaks: 40.0 ± 0.9 Å (n = 3 experiments) for 6,7-BRPC; 39.5 ± 0.9 Å (n = 5) for 11,12-BRPC; 41.6 ± 0.3 Å (n = 5) for 15,16-BRPC; and 39.0 Å (n = 1) for POPC. The medium electron density regions at the outer edges of each profile correspond to the water layers between adjacent bilayers. The regions of the profiles between the head-group peaks and the center of the bilayer correspond to the lipid methylene chains. Clearly, the shape and relative density of the methylene chain regions depend on the position of the bromine atoms along the hydrocarbon chain. For the control POPC bilayer, with no bromine present, the methylene chain region is at an intermediate density between the head-group peak and the low-density trough in the geometric center of the bilayer which corresponds to the localization of the lipid methyl groups. For 6,7-BRPC, there are additional high-density peaks, presumably caused by the bromine atoms, located at about ±13 Å. For 11,12-BRPC, the additional high-density peaks in the profile caused by the bromine are centered at about ±7 Å. This profile is similar in shape to profiles calculated for 1-palmitoyl-2-bromopalmitoyl-PC, where the *sn*-2 chain is brominated at either the C-9 or the C-10 position (Lytz et al., 1984). In the 15,16-BRPC profile, the terminal methyl trough is replaced by a broad peak centered at the origin. Thus, the location of the high-density bromine peaks is a function of the position of the bromine atoms on the hydrocarbon chain.

To determine as accurately as possible structural changes produced by the incorporation of bromine, we performed modeling studies. The first objective was to see if the observed changes in continuous transform (Figure 1) could be modeled by simply adding electron density, due to the bromine atoms, at discrete positions in the POPC bilayer. The electron density distribution of the bromine atoms was modeled in a manner similar to that of Franks et al. (1978). It was assumed that the pair of bromine atom in each labeled hydrocarbon chain could be approximated by two Gaussian distributions of height B, width σ, and distances $+s$ and $-s$ from the bilayer center. That is, the bromine atoms in the bilayer were approximated by an electron density function

$$\rho_{Br}(x) = B \exp\{-[(x + s)/\sigma]^2\} + B \exp\{-[(x - s)/\sigma]^2\} \quad (1)$$

whose Fourier transform is

$$F_{Br}(X) = 2B\sqrt{\pi}\sigma \exp[-(X\pi\sigma)^2] \cos(2\pi Xs) \quad (2)$$

The procedure was to determine if the parameters B, σ, and s could be chosen so that when $F_{Br}(X)$ was added to the POPC continuous transform, $F_{POPC}(X)$, it would produce transforms similar to the experimental transforms of Figure 1. The height of the Gaussian, B, was chosen so that experimental and model transforms matched at the origin of reciprocal space. The parameters σ and s were varied in increments of 1 and $^1/_2$ Å, respectively, until the best match of experimental and continuous transforms was obtained. This match was more sensitive to variations in s than to variations in σ. Figure 3 shows the continuous transforms $F_{Br}(X)$ and $F_{POPC}(X)$ and the total transform

$$F_{T_1}(X) = F_{POPC}(X) + F_{Br}(X) \quad (3)$$

that gave the best fits to the experimental transforms of Figure 1. Figure 4 shows the model transforms, $F_{T_1}(X)$, compared to the experimental transforms for 6,7-BRPC, 11,12-BRPC,

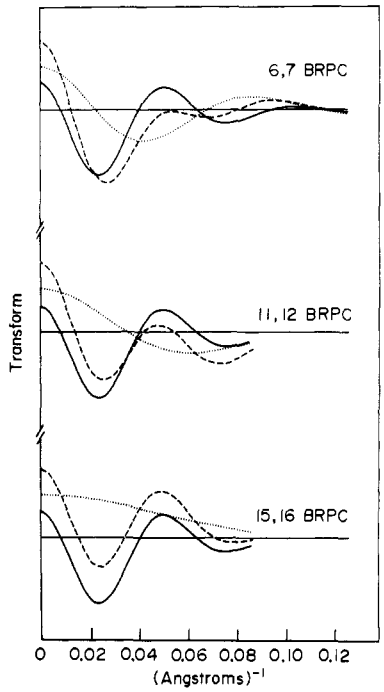

FIGURE 3: Continuous transforms for POPC (solid lines), bromine atoms in the bilayer (dotted lines), and total calculated transform, $F_{T_1}(X) = F_{POPC}(X) + F_{Br}(X)$ (dashed lines). In $F_{Br}(X)$, the distance of the bromine peaks from the bilayer center, s, is 11, 6.5, and 2 Å for 6,7-, 11,12-, and 15,16-BRPC, respectively.

and 15,16-BRPC. For each of the three model transforms, σ was 4 Å. The best fits for $F_{T_1}(X)$ to the experimental transforms were s = 11, 6.5, and 2 Å for 6,7-BRPC, 11,12-BRPC, and 15,16-BRPC, respectively.

In general, this simple modeling procedure was able to approximate the shapes of the observed transforms for 6,7-BRPC and 11,12-BRPC (Figure 4). However, there was significant mismatch between the model and experimental transforms for 15,16-BRPC (Figure 4). That is, no choice of σ and s was able to produce a model transform $F_{T_1}(X)$ which matched closely the experimental transform for 15,16-BRPC. The most likely explanation for this discrepancy is that the width of the bilayer is greater for 15,16-BRPC than for POPC, as indicated by the electron density profiles (Figure 1). To test this idea, a second set of modeling experiments was performed. In this procedure, we set

$$F_{T_2}(X) = F_{Br}(X) + F_{ST}(X) \quad (4)$$

where $F_{Br}(X)$ is the same function as defined in eq 2, and $F_{ST}(X)$ is the Fourier transform of a one-dimensional electron density strip model (Worthington, 1969). Strip models have often been used in diffraction analysis of membranes and lipid bilayers (Worthington & Blaurock, 1969; Franks et al., 1982; King et al., 1984; McDaniel & McIntosh, 1986). The strip model we chose has five uniform density strips corresponding to the terminal methyl region in the center of the bilayer, two methylene chain regions, and two head-group regions. We started with strip widths and densities similar to previous studies (Franks et al., 1982; King et al., 1984; McDaniel & McIntosh, 1986) and then varied the bilayer width by systematically changing the thickness of the strip corresponding to the methylene chain region of the bilayer in increments of $^1/_2$ Å. The electron densities and widths of the other strips were kept constant and are given in the legends to Figure 5. The bilayer parameters obtained from these calculations are shown in Table I. Comparisons of the observed and model transforms as calculated from eq 4 are shown in Figure 5. We

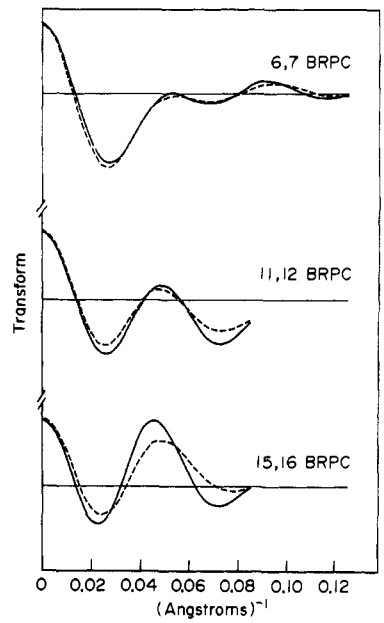

FIGURE 4: Observed (solid lines) and calculated transforms, $F_{T_1}(X)$ (dashed lines), for 6,7-BRPC, 11,12-BRPC, and 15,16-BRPC.

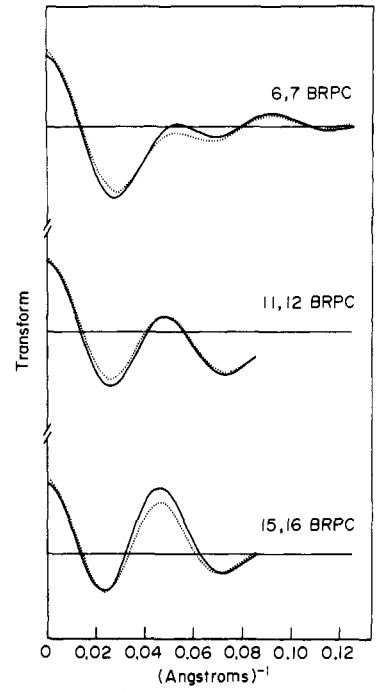

FIGURE 5: Observed (solid lines) and calculated transforms, $F_{T_2}(X)$ (dotted lines), for 6,7-BRPC, 11,12-BRPC, and 15,16-BRPC. Electron density strip models were used to calculate $F_{T_2}(X)$. All models have five uniform density strips corresponding to the terminal methyl region, two methylene chain regions, and two head-group regions, with electron densities of 0.25, 0.32, and 0.44 electron/Å^3, respectively. For 6,7- and 11,12-BRPC, the widths are 7, 11, and 10 Å for the terminal methyl, methylene chain, and head-group regions, respectively. For 15,16-BRPC, the widths for these three strips are 7, 12.5, and 10 Å.

used the values of σ and s as shown in Figure 3. The closest agreement between experimental and model transforms is obtained when the total bilayer thickness, d_b, is equal to 49, 49, and 52 Å for 6,7-BRPC, 11,12-BRPC, and 15,16-BRPC, respectively. For each of these lipids, the total bilayer thickness, as estimated by the electron density strip models, is about 10 Å larger than the head-group peak separation in the electron density profile (Figure 2). Thus, both the electron density profiles and this model calculation indicate that the bilayer thickness depends on the location of the bromine atoms,

Table I: Bilayer Dimensions

lipid	bilayer thickness, d_b (Å)	hydrocarbon thickness, d_{hc} (Å)	bromine distance from bilayer center, s (Å)	bromine distance from head-group/hydrocarbon boundary, $(d_{hc}/2) - s$ (Å)
POPC	49	29		
6,7-BRPC	49	29	11.0	3.5
11,12-BRPC	49	29	6.5	8.0
15,16-BRPC	52	32	2.0	14.0

with the bilayer being widest in 15,16-BRPC, where the bromines are near the terminal methyl end of the chain.

Discussion

Both the electron density profiles (Figure 2) and the model calculations (Figures 3–5 and Table I) provide three pieces of information which should be useful for experiments where brominated lipids are used as probes. First, the bilayers formed from BRPCs are similar in structure to bilayers made from unbrominated lipids, such as POPC. As measured both by head-group peak separation in the electron density profile and as total width of the strip models (Table I), the bilayer thicknesses for POPC, 6,7-BRPC, and 11,12-BRPC are approximately the same, to within about 1 Å, whereas 15,16-BRPC forms bilayers which are about 3 Å thicker. Second, the bromine atoms appear to be well localized in the bilayer interior. Discrete peaks appear in electron density profiles for 6,7-BRPC and 11,12-BRPC which are caused by the presence of the bromine atoms (Lytz et al., 1984). For 15,16-BRPC, a single high-density bromine peak is observed centered at the geometric center of the bilayer. In this case, bromine labels from apposing monolayers are close enough that the individual peaks for each monolayer are not resolved in the profile. The modeling calculations indicate that for 15,16-BRPC the bromine labels are only about 2 Å from the geometric center of the bilayer (Table I), so that the bromines from apposing monolayers are separated by 4 Å, less than the resolution of the electron density profiles, $d/2h_{max} \simeq 7$ Å. The modeling studies quantitatively show that the bromine labels are well localized, as they indicate for each of the three lipids that the half-width of the bromine peak is about 4 Å. Lytz et al. (1984) calculated, on the basis of the radius of Br and the distance between adjacent positions on the hydrocarbon chains, that the projected width of the pair of bromine atoms on each chain should be about 3.9 Å. Third, this analysis gives accurate estimates for the location of the bromine labels for the three lipids (Table I). The electron density profiles and model calculations are in general agreement on the location of the labels. However, the modeling calculations give more reliable estimates of the positions of the labels since in the electron density profiles the label peaks overlap in the case of 15,16-BRPC, as discussed above, and the head group and bromine peaks partially overlap in the case of 6,7-BRPC (Figure 2). The model calculations are also preferable in comparing the structural parameters for the different lipids, since the profile for 6,7-BRPC is at a higher resolution than the other profiles. In Table I, the right-hand column gives the distance from the center of the Gaussian distribution for each pair of bromine atoms (eq 1) to the edge of the boundary between the head-group and methylene chain regions in the electron density strip model. The location of this boundary relative to the bromolipid molecules is difficult to define precisely, although previous extensive model studies have shown that, for dioleoylphosphatidylcholine in the liquid-crystalline phase, the boundary occurs near the C-2 carbon (King & White, 1986).

The dimensions presented in Table I provide further information on the structure of these liquid-crystalline bilayers. For instance, consider the distance of the bromine atoms from either the bilayer center or the head-group/hydrocarbon boundary. The difference in both of these distances between 6,7-BRPC and 11,12-BRPC is 4.5 Å, or an incremental distance of 0.9 Å per CH_2 group. This is in excellent agreement with the results of Lewis and Engleman (1983), who measured bilayer thickness of liquid-crystalline PCs, one series with both acyl chains saturated and the other series with both acyl chains monounsaturated. For both of these classes of lipids, they found an increment in bilayer thickness of about 0.9 Å/CH_2 group [see Figure 3 of Lewis & Engleman (1983)]. Thus, for both 6,7-BRPC and 11,12-BRPC, the thickness per CH_2 of the *sn*-2 chain group is typical for liquid-crystalline bilayers.

The situation is more complicated in the case of 15,16-BRPC for two reasons. First of all, the bilayer thickness is greater for 15,16-BRPC than for 6,7-BRPC, 11,12-BRPC, or POPC. Second, the difference in distance between the position of the bromines in 15,16-BRPC and in 6,7-BRPC (or 11,12-BRPC) is different as measured from the bilayer center than as measured from the head-group/hydrocarbon boundary (see Table I). For example, the difference in distance between the bromines in 11,12-BRPC and 15,16-BRPC is 4.5 Å as measured from the bilayer center and 6.0 Å as measured from the head-group/hydrocarbon boundary. The most likely reason for this difference is that in 15,16-BRPC there is less disorder in the hydrocarbon chain packing from the head group to the bromine atoms than there is from the bromine atoms to the center of the bilayers. The data are not sufficient to completely specify the chain packing in 15,16-BRPC. However, by using some reasonable assumption, we can make a rough calculation of the incremental width per CH_2 group in 15,16-BRPC. We assume the following: (1) the head-group conformation is similar for all of the bromolipids, so that the head-group/hydrocarbon interface is in the same position along the *sn*-2 chain for 6,7-, 11,12-, and 15,16-BRPC; (2) the hydrocarbon chains do not interdigitate in the center of the bilayer; (3) the distance between apposing terminal methyl groups is twice the separation of adjacent methylenes, since, in the liquid-crystalline state, the volume of a CH_3 group is about twice the volume of a CH_2 group (Blaurock & Nelander, 1979); and (4) the centers of the mass of the bromine atoms for 6,7-, 11,12-, and 15,16-BRPC are at carbons 6.5, 11.5, and 15.5, respectively. Using our previous result that the increment per CH_2 group is 0.9 Å/CH_2 for both 6,7- and 11,12-BRPC, we can set up equations to determine the increment per CH_2 for 15,16-BRPC. As measured from the bilayer center, the separation between bromine peaks for 6,7-BRPC and 15,16-BRPC is given by

$$12.5(0.9 \text{ Å}/CH_2) - 3.5Y = 9 \text{ Å} \quad (5)$$

and the separation between bromine peaks for 11,12-BRPC and 15,16-BRPC is given by

$$7.5(0.9 \text{ Å}/CH_2) - 3.5Y = 4.5 \text{ Å} \quad (6)$$

where Y is the increment per CH_2 group for 15,16-BRPC as measured from the bilayer center. Note that, following as-

sumption 3, we have added an extra CH_2 increment to correspond to the distance between the terminal methyl group and the bilayer center. Both eq 5 and eq 6 are solved by $Y = 0.64$ Å/CH_2. Next, consider the separation between bromine peaks relative to the head-group/hydrocarbon interface. Using the calculated value of 0.9 Å/CH_2 for both 6,7- and 11,12-BRPC, we find that for both of these lipids the interface is located between carbons C-2 and C-3. Assuming the interface is in the same location for 15,16-BRPC, we calculate that 6,7-, 11,12-, and 15,16-bromine atoms are 3.9, 8.9, and 12.9 CH_2 groups from the interface. Therefore, if we let Z = the increment per CH_2 group of the 15,16-bromine atoms from the head-group/hydrocarbon interface, the difference in distance from this interface for 6,7- and 15,16-BRPC is given by

$$12.9Z - 3.9(0.9 \text{ Å}/CH_2) = 10.5 \text{ Å} \quad (7)$$

and for 11,12- and 15,16-BRPC is given by

$$12.9Z - 8.9(0.9 \text{ Å}/CH_2) = 6.0 \text{ Å} \quad (8)$$

Both eq 7 and eq 8 are solved by $Z = 1.09$ Å/CH_2. Thus, these calculations lead to a packing model for 15,16-BRPC where the increment per CH_2 group from the head group to the bromine atoms is about 1.1 Å/CH_2, whereas the increment per CH_2 group from the bromine atoms to the bilayer center is only about 0.6 Å/CH_2. These numbers can be compared to the increments for a typical liquid-crystalline lipid of about 0.9 Å/CH_2 (Lewis & Engelman, 1983) and for a gel-state lipid of 1.25 Å/CH_2. Thus, in 15,16-BRPC, there is relatively ordered packing from the head group to the bromine atoms, with quite disordered chain packing in the center of the bilayer. The more orderly (more "gel-like") packing for most of the hydrocarbon chain region would explain why 15,16-BRPC forms a wider bilayer and melts at a higher temperature in comparison to POPC, 6,7-BRPC, and 11,12-BRPC.

Our observations on bilayer widths as a function of position of the bromine labels can be related to previous studies. Barton and Gunstone (1975) found, for a series of positional isomers of 1,2-dioctadecenoyl-*sn*-phosphatidylcholines, that the main transition temperature, enthalpy of transition, and spin–lattice relaxation times depend strongly on the position of the double bond. They found enhanced molecular motion about the middle of the chain and, in particular, found that the degree of disorder of the lipid chains is greater when the double bond is in the 9,10-position than when it is in the 4,5- or 15,16-positions (Barton & Gunstone, 1975). Previous studies on bilayers have shown that the bilayer width decreases above the phase transition, over and above that decrement due to a change in the angle of tilt of the lipid chains to the bilayer normal, as the chains become more disordered (Seelig & Seelig, 1974; Zaccai et al., 1979), and that lipids with unsaturated chains are more disordered (Levine et al., 1972) and have a smaller bilayer width than bilayers of fully saturated lipids (Lewis & Engelman, 1983). Therefore, our observation that the bilayer width for 15,16-BRPC is greater than that of either 6,7-BRPC or 11,12-BRPC is expected from the placement of the perturbing bromine atoms closer to the end of the acyl chain rather than near the middle of the chain.

Registry No. 6,7-BRPC, 81138-96-7; 11,12-BRPC, 96110-16-6; 15,16-BRPC, 96110-17-7.

REFERENCES

Barton, P. G., & Gunstone, F. D. (1975) *J. Biol. Chem. 250*, 4470–4476.

Blatt, E., & Sawyer, W. H. (1985) *Biochim. Biophys. Acta 822*, 43–62.

Blaurock, A. E., & Nelander, J. C. (1979) *J. Neurochem. 32*, 1753–1760.

Blaurock, A. E., & McIntosh, T. J. (1986) *Biochemistry 25*, 299–305.

Boss, W. F., Kelley, C. J., & Landsberger, F. (1975) *Anal. Biochem. 64*, 259–292.

Deisenhofer, J., Epp, O., Miki, K., Huber, R., & Michel, H. (1985) *Nature (London) 318*, 618–624.

East, J. M., & Lee, A. G. (1982) *Biochemistry 21*, 4144–4151.

Eisenberg, D. (1984) *Annu. Rev. Biochem. 53*, 595–623.

Everett, J., Zlotnick, A., Tennyson, J., & Holloway, P. W. (1986) *J. Biol. Chem. 261*, 6725–6729.

Franks, N. P., Arunanachalam, T., & Caspi, E. (1978) *Nature (London) 276*, 530–532.

Franks, N. P., Melchior, V., Kirschner, P. A., & Caspar, D. L. D. (1982) *J. Mol. Biol. 155*, 133–153.

Gogol, E. P., & Engelman, D. M. (1984) *Biophys. J. 46*, 491–495.

Hitchcock, P. B., Mason, R., Thomas, K. M., & Shipley, G. G. (1974) *Proc. Natl. Acad. Sci. U.S.A. 71*, 3036–3040.

Jain, M. K., & Maliwal, B. P. (1985) *Biochim. Biophys. Acta 814*, 135–140.

King, G. I., & Worthington, C. R. (1971) *Phys. Lett. A 35A*, 259.

King, G. I., & White, S. H. (1986) *Biophys. J. 49*, 1047–1054.

King, G. I., Chao, N., & White, S. H. (1984) in *Neutrons in Biology* (Schoenborn, B. P., Ed.) pp 159–172, Plenum Press, New York.

Kleinfeld, A. M. (1985) *Biochemistry 24*, 1874–1882.

Levine, Y. K., Birdsall, J. M., Lee, A. G., & Metcalfe, J. C. (1972) *Biochemistry 11*, 1416–1421.

Lewis, B. A., & Engelman, D. M. (1983) *J. Mol. Biol. 166*, 211–217.

London, E. (1982) *Mol. Cell. Biochem. 45*, 181–188.

Lüdi, H., Hasselbach, W., & Gaugler, H. (1985) *Biochim. Biophys. Acta 814*, 120–124.

Lytz, R. K., Reinert, J. C., Church, S. E., & Wickman, H. H. (1984) *Chem. Phys. Lipids 35*, 63–76.

Markello, T., Zlotnick, A., Everett, J., Tennyson, J., & Holloway, P. W. (1985) *Biochemistry 24*, 2895–2901.

McDaniel, R. V., & McIntosh, T. J. (1986) *Biophys. J. 49*, 94–96.

McIntosh, T. J. (1980) *Biophys. J. 29*, 237–246.

McIntosh, T. J., & Simon, S. A. (1986) *Biochemistry 25*, 4058–4066.

McIntosh, T. J., McDaniel, R. V., & Simon, S. A. (1983) *Biochim. Biophys. Acta 731*, 109–114.

McIntosh, T. J., Simon, S. A., Ellington, S. C., & Porter, N. A. (1984) *Biochemistry 23*, 4038–4044.

Rzepecki, L. M., Strittmatter, P., & Herbette, L. G. (1986) *Biophys. J. 49*, 829–838.

Seelig, A., & Seelig, J. (1974) *Biochemistry 13*, 4839–4845.

Shannon, C. E. (1949) *Proc. Inst. Radio Eng. N.Y. 37*, 10–21.

Smith, R., & Oldfield, E. (1984) *Science (Washington, D.C.) 225*, 280–288.

Storch, J., & Kleinfeld, A. M. (1986) *Biochemistry 25*, 1717–1726.

Tardieu, A., Luzzati, V., & Reman, F. C. (1973) *J. Mol. Biol. 75*, 711–733.

Torbet, J., & Wilkins, M. H. F. (1976) *J. Theor. Biol. 62*, 447–458.

Worthington, C. R. (1969) *Biophys. J. 9*, 222–234.

Worthington, C. R., & Blaurock, A. E. (1969) *Biophys. J. 9*, 970–990.

Worthington, C. R., King, G. I., & McIntosh, T. J. (1973) *Biophys. J. 13*, 480–494.

Zaccai, G., Büldt, G., Seelig, A., & Seelig, J. (1979) *J. Mol. Biol. 134*, 693–706.